ResearchGate

See discussions, stats, and author profiles for this publication at: https://www.researchgate.net/publication/231530582

Time-Resolved In-Situ Energy and Angular Dispersive X-ray Diffraction Studies of the Formation of the Microporous Gallophosphate ULM-5 under Hydrothermal Conditions

ARTICLE *in* JOURNAL OF THE AMERICAN CHEMICAL SOCIETY · JANUARY 1999

Impact Factor: 12.11 · DOI: 10.1021/ja982441c

CITATIONS
102

READS
17

7 AUTHORS, INCLUDING:

Stephen O'Brien
City College of New York
126 PUBLICATIONS **7,688** CITATIONS
SEE PROFILE

Shiv Halasyamani
University of Houston
266 PUBLICATIONS **5,665** CITATIONS
SEE PROFILE

Dermot O'Hare
University of Oxford
391 PUBLICATIONS **10,126** CITATIONS
SEE PROFILE

Gérard Férey
Université de Versailles Saint-Quentin
705 PUBLICATIONS **36,600** CITATIONS
SEE PROFILE

Available from: Stephen O'Brien
Retrieved on: 16 January 2016

Time-Resolved In-Situ Energy and Angular Dispersive X-ray Diffraction Studies of the Formation of the Microporous Gallophosphate ULM-5 under Hydrothermal Conditions

Robin J. Francis,[†] Stephen O'Brien,[†] Andrew M. Fogg,[†] P. Shiv Halasyamani,[†] Dermot O'Hare,*[,†] Thierry Loiseau,[‡] and Gerard Férey[‡]

Contribution from the Inorganic Chemistry Laboratory, University of Oxford, South Parks Road, Oxford OX1 3QR, U.K., and Institu Lavoisier, IREM UMR C 173, Université de Versailles, 45 Avenue des Etat-Unis, 78035 Versailles, France

Received July 10, 1998

Abstract: The hydrothermal synthesis of the large-pore oxy-fluorinated gallophosphate ULM-5 has been followed in situ using time-resolved energy dispersive and angular dispersive X-ray diffraction. A variety of synthetic parameters such as temperature, reagent stoichiometry, source materials, and pH have been studied, and their effect on the crystallization determined. The nature of the phosphorus source used, either orthophosphoric acid or phosphorus pentoxide, is found to have a profound influence on the reaction pathway. Using orthophosphoric acid, ULM-5 is found to form very rapidly following a short induction period. A kinetic analysis of the crystallization of ULM-5 using orthophosphoric acid under isothermal hydrothermal conditions has been performed. Comparison of the experimentally determined extent of reaction (α) versus time data with those predicted by various theoretical models indicates that over a wide range of temperatures and pH the crystallization can be modeled by a three-dimensional diffusion-controlled process. This process occurs at a rate essentially independent of temperature and pH. In contrast, using phosphorus pentoxide, the formation of ULM-5 is found to proceed via the formation of either of two distinct crystalline intermediate phases, which subsequently react to form the ULM-5 final product at a rate which is strongly dependent on temperature. The relative quantities of each intermediate phase formed depend critically on the precise reagent stoichiometry used. Conditions have been identified in which ULM-5 can be formed exclusively via either intermediate phase. The mechanism of transformation of intermediate to product phases appears to be either a direct solid−solid transformation, or via the dissolution or amorphorization of only a small quantity of material at the surface of the intermediate crystallites.

Introduction

Understanding the mechanisms by which microporous materials, crystalline materials containing ordered arrays of regularly sized and shaped pores and channels of molecular dimensions, are synthesized under hydrothermal conditions has been described as one of the greatest challenges facing today's experimental chemists.[1] Hydrothermal crystallizations are multicomponent heterogeneous reactions in which a plethora of interactions, chemical equilibria, reactions, and nucleation and growth processes are taking place throughout the reaction medium, many of which are interdependent and change with time.[2,3] To further complicate matters, it has been conclusively demonstrated that there is no universal crystallization mechanism for molecular sieves; different molecular sieves crystallize via different mechanisms, and the same molecular sieve can be crystallized via different mechanisms depending on the reaction conditions employed.[4,5] Hence, although careful experimental studies have revealed details of the mechanisms by which particular molecular sieves are synthesized under certain specific reaction conditions,[6−9] in general, the complexity of hydrothermal crystallizations has led to great difficulty in trying to ascertain the details of the processes occurring during the formation of these materials. Although progress has recently been made,[10,11] the lack of a fundamental understanding of the mechanisms by which molecular sieves are formed means that, in general, the rational a priori design of a new molecular sieve material with predesigned physical properties remains an elusive goal in solid-state materials chemistry. Consequently, to date, the synthesis of new molecular sieve materials has been a mainly heuristic exercise involving the systematic exploration of a very large *n*-dimensional reaction space. Besides being time-consuming and inefficient, such a process requires a large degree of serendipity for the successful synthesis of new, pure phase materials, and the degree of control over the physical properties of the synthesized phase is limited at best. This is unfortunate

[†] University of Oxford.
[‡] Université de Versailles.

(1) Lok, B. M.; Cannon, T. R.; Messina, C. A. *Zeolites* **1983**, *3*, 282−291.
(2) Davis, M. E.; Lobo, R. F. *Chem. Mater.* **1992**, *4*, 756−768.
(3) Francis, R. J.; O'Hare, D. *J. Chem. Soc., Dalton Trans.* **1998**, 3133−3148.
(4) Iton, L. E.; Trouw, F.; Brun, T. O.; Epperson, J. E. *Langmuir* **1992**, *8*, 1045−1048.
(5) Bodart, P.; Nagy, J. B.; Gabelica, Z.; Derouane, E. G. *J. Chim. Phys. Phys.-Chim. Biol.* **1986**, *83*, 777.
(6) Burkett, S. L.; Davis, M. E. *Chem. Mater.* **1995**, *7*, 920−928.
(7) Burkett, S. L.; Davis, M. E. *Chem. Mater.* **1995**, *7*, 1453−1463.
(8) Schoeman, B. J.; Sterte, J.; Otterstedt, J. E. *Zeolites* **1994**, *14*, 568−575.
(9) Dutta, P. K.; Shieh, D. C. *J. Phys. Chem.* **1986**, *90*, 2331−2334.
(10) Willock, D. J.; Lewis, D. W.; Catlow, C. R. A.; Hutchings, G. J.; Thomas, J. M. *J. Mol. Catal., A* **1997**, *119*, 415−424.
(11) Lewis, D. W.; Sankar, G.; Wyles, J. K.; Thomas, J. M.; Catlow, C. R. A.; Willock, D. J. *Angew. Chem., Int. Ed. Engl.* **1997**, *36*, 2675−2677.

10.1021/ja982441c CCC: $18.00 © 1999 American Chemical Society
Published on Web 01/26/1999

given the very broad range of industrially and academically important materials chemistry applications, including heterogeneous catalysis,[12] ion exchange, and gas separation, for which these materials are used. A more thorough understanding of the kinetic and mechanistic processes occurring during the synthesis of these materials leading to more rational, targeted syntheses would therefore be of great value.

A very powerful and efficient way of probing the processes occurring during the formation of microporous phases is to perform in situ studies of their formation in real time, under actual laboratory synthetic conditions.[3,13] In situ studies have two major advantages over conventional "ex situ" studies that involve the periodic quenching of the reaction, followed by product workup and analysis. First, in situ techniques allow reactions to be studied under *normal laboratory reaction conditions*. This avoids the constant concern with ex situ experiments that the reaction may be affected by the workup and analysis process, and that the species observed in these experiments are not representative of the species present in the reaction mixture at the time of quenching. Second, in situ experiments allow the continuous monitoring of the syntheses, thus vastly increasing the quantity of data obtained per reaction relative to ex situ experiments which provide relatively few data. This advantage is of particular importance given the lack of a universal crystallization mechanism referred to earlier, which has the consequence that each system and set of reaction conditions must be studied individually—a laborious and time-consuming process using ex situ techniques. Further advantages of in situ techniques include the ability to directly observe the formation of intermediate phases and their transformation to the product phase, the much increased time resolution, and the ready ease with which the effect of changing reaction conditions can be assessed. The application of in situ techniques to the study of hydrothermal crystallizations has recently been reviewed both by ourselves and by others.[3,13]

We have been interested in studying the kinetics and mechanisms of the formation of microporous materials by in situ diffraction techniques, and have described the development of a facility using energy-dispersive X-ray diffraction (EDXRD) for use on station 16.4 of the Synchrotron Radiation Source (SRS), Daresbury Laboratory, U.K.[14] Recently we have been studying the synthesis of a family of microporous oxyfluorinated gallophosphates synthesized by Férey and coworkers[15,16] denoted ULM-*n* (where *n* is an integer referring to the order of discovery). Our in situ XRD studies on the ULM-*n* family of materials have to date focused on one particular member, ULM-5. We report here a detailed study of the synthesis of ULM-5 under a variety of conditions of temperature, pH, reaction composition, and source material using in situ energy dispersive and angular dispersive X-ray diffraction.

Experimental Section

Synthesis. ULM-5 was synthesized in a manner similar to those described previously.[17] Reaction mixtures of composition $1Ga_2O_3$:xP_2O_5:1HF:1DAH:yH_2O (DAH = 1,6-diaminohexane), where $x = 0.9-2.5$ and $y = 80-240$, were reacted under isothermal hydrothermal conditions at autogenous pressures. Precise reaction conditions and stoichiometries for each experiment are detailed explicitly in the text at the appropriate points. In general all syntheses were performed in exactly the same way each time, although the experimental procedure used depended on the form of the phosphorus source. Using orthophosphoric acid, the appropriate quantity of gallium oxide (Aldrich, 99.99%) was added, with stirring, to a separately mixed solution of the aqueous phosphoric acid (BDH, 85%), aqueous hydrofluoric acid (BDH, 40%), and water. The solid 1,6-diaminohexane (Lancaster, 98%) was added last, immediately prior to sealing the cell and beginning the reaction. If phosphorus pentoxide was being used, the procedure was modified slightly; in this case the phosphorus pentoxide (BDH) was added last, after the 1,6-diaminohexane, immediately prior to reaction. Typically the total amount of reagents used in each reaction was 1−1.5 g of solid and 10−15 mL of solution. After mixing of the reagents the cell was immediately sealed and introduced to the block, which had been previously heated to the desired reaction temperature. The cell was then kept at this temperature for the remainder of the reaction. In general, the delay from mixing to introduction of the cell to the block was on the order of 3 min, and data collection was begun less than 1 min later.

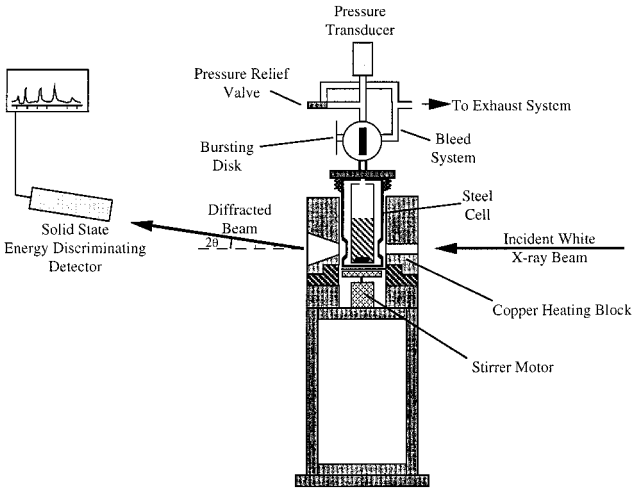

Figure 1. Schematic diagram of the experimental apparatus used to study hydrothermal reactions in situ using time-resolved energy dispersive X-ray diffraction on station 16.4 of the SRS, Daresbury Laboratory, U.K.

Energy Dispersive Diffraction Experiments. Time-resolved energy dispersive X-ray diffraction (EDXRD) experiments were performed on station 16.4 of the U.K. SRS at Daresbury Laboratory. Reactions were performed in a hydrothermal pressure cell which we had previously designed for studying hydrothermal reactions using energy dispersive radiation.[14] In this system a large-volume (ca. 30 cm^3) stainless steel reaction cell is loaded with reagents, sealed, and heated to the desired reaction temperature under autogenous pressure. The main reaction cell consists of a modified Parr Instruments stainless steel autoclave and gauge block assembly. Over a 29 mm height range of the cell the wall thickness has been machined down to 0.4 mm to allow entry and exit of the incident and diffracted beam with minimum loss of intensity. The very high intensity of radiation available from synchrotron sources in energy dispersive mode allows the X-ray radiation to penetrate the reaction cell and enables the collection of high-quality spectra using acquisition times on the order of seconds. Accurate temperature control is achieved by placing the reaction cell in a solid aluminum block equipped with cartridge heaters attached to a PID temperature controller. A schematic diagram of the experimental apparatus is shown in Figure 1. A detailed technical report of the design of the cell and the sample environment control system has been previously published elsewhere.[14]

Station 16.4 receives X-ray radiation from a wiggler magnet operating at a peak field of 6 T. The usable X-ray flux is continuous in the range 5−120 keV, with a maximum X-ray flux of 3×10^{10} photon/s at approximately 13 keV. The position of the maximum intensity at the detector is, however, shifted to higher energy on introduction of the experimental apparatus, due to the absorption of

(12) Venuto, P. B. *Microporous Mater.* **1994**, *2*, 297−411.
(13) Cheetham, A. K.; Mellot, C. F. *Chem. Mater.* **1997**, *9*, 2269−2279.
(14) Evans, J. S. O.; Francis, R. J.; O'Hare, D.; Price, S. J.; Clarke, S. M.; Flaherty, J.; Gordon, J.; Nield, A.; Tang, C. C. *Rev. Sci. Instrum.* **1995**, *66*, 2442−2445.
(15) Ferey, G.; Loiseau, T.; Riou, D. *Mater. Sci. Forum* **1994**, *152*−*153*, 125−130.
(16) Ferey, G. *J. Fluorine Chem.* **1995**, *72*, 187−193.
(17) Loiseau, T.; Ferey, G. *J. Solid State Chem.* **1994**, *111*, 403−415.

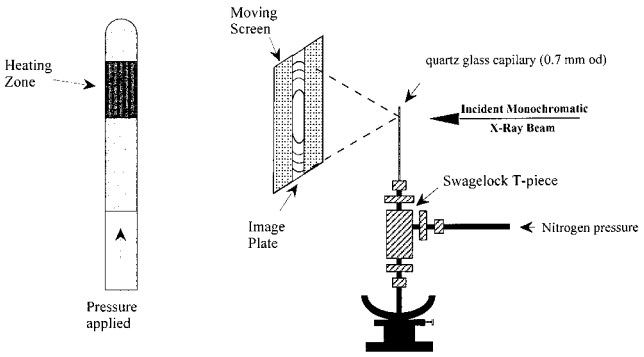

Figure 2. Schematic diagram of the experimental apparatus used to study hydrothermal reactions in situ using time-resolved angular dispersive X-ray diffraction on station X7B of the NSLS, Brookhaven National Laboratory.

lower energy photons by the cell materials. Useful intensity could be obtained above ca. 40 keV. After diffraction by the sample the diffracted beam passes through a set of parallel collimating slits and then onto an EG&G ORTEC solid-state detector. Data acquisition is based on the "Pincer" program which provides a command interpreter and a large number of functions using macro command files. The station electronics and data collection software were configured so that a series of spectra could be recorded during the course of a reaction. Further details of the station design, the energy dispersive technique, and the station electronics and data collection software are described in more detail elsewhere.[18−22] Acquisition times were chosen to be short enough to be appropriate for time-resolved studies while still giving high-quality individual spectra suitable for the accurate extraction of reflection intensities. In practice, acquisition times of 30−60 s were used.

Since the energy E (keV) at which a Bragg reflection from planes of separation d (Å) is given by E (keV) = 6.19926/(d sin θ), a detector angle of 1.20−1.25° (2θ) was chosen for all experiments, which, given the energy profile of the radiation available on station 16.4 taking into account the absorption due to the cell, gives an observable d spacing range of ca. 5−16 Å. The highest observed d spacing in ULM-5 is 14.4 Å.[17]

The reactions were performed under isothermal conditions. Accurate temperature control (±1 °C) was achieved using the heating block and control system previously described.[14] The reactions were performed by introducing the reaction cell to the preheated block. Introduction of the cold thermal mass of the cell to the block causes an initial drop in the temperature of the block of ca. 20 °C and consequent small deviations from isothermal conditions. However, equilibration of the block−cell assembly to the reaction temperature typically took less than 5 min, shorter than the induction times seen in these reactions.

Angular Dispersive Diffraction Experiments. Angular dispersive diffraction (ADXRD) experiments were performed on station X7B of the National Synchrotron Radiation Source at Brookhaven National Laboratory.[23−26] Aliquots of a reaction mixture prepared as described above were syringed into 0.7 mm quartz glass capillaries using a thinner capillary mounted on a syringe. The capillaries were mounted on a Swagelock fitting with a Vespel ferrule as shown in Figure 2. Pressure was applied externally from a nitrogen cylinder to a pressure in excess of the autogenous pressure of water at the reaction temperature. Typically the pressure applied was on the order of 20 bar. Heating of the reaction mixture to the desired temperature was achieved by applying a hot air steam to a small zone of the capillary as shown in Figure 2. The heated zone was approximately 5 mm while the X-ray beam was defined by slits to be 2 × 0.7 mm. The X-ray beam was defined to be smaller than the heated zone to reduce problems of temperature gradients and convection and diffusion. To try to eliminate problems of sample settling and preferred orientation, the sample was oscillated through an angle of 90° during the reaction. Further details of the experimental technique have been published elsewhere.[23−26]

The detector used for collection of the powder diffraction patterns was a Translating Image Plate camera specially constructed for time-, temperature-, and wavelength-dependent powder diffraction experiments.[23] A 200 × 400 mm Fuji imaging plate was translated behind a steel screen containing a 3 mm vertical slit. In this way a continuous set of powder diffraction patterns was recorded. The individual pixel size on the image plates is 0.1 × 0.1 mm. There are therefore 2000 individual pixels in the direction that the image plate is scanned. For the purposes of data analysis the image plate was divided into 3.0 mm wide strips by adding 30 pixels. Each experiment was performed over a period of 3 h. Each strip therefore corresponds to ca. 3 min of time.

Before reaction, accurate values for the wavelength, zero point correction, and image plate tilt were obtained using a LaB_6 standard (NIST No. 660).[25] Corrections were also made for fluctuations and decay of the incident X-ray beam by using monitor counts collected between the incident beam defining slit and the sample.

Results

ULM-5 was synthesized according to published techniques using reaction mixtures of composition $1Ga_2O_3$:xP_2O_5:yHF:zDAH:nH$_2$O (DAH = 1,6-diaminohexane), where x = 0.9−2.5, y = 1.7−2.3, z = 0.85−1.15, and n = 80−240. The phosphorus source used was either orthophosphoric acid (H_3PO_4) or phosphorus pentoxide (P_2O_5). Early in our studies we discovered that the nature of the phosphorus source had a dramatic effect on the pathway of the reaction.[27] For this reason it is convenient to discuss the results in two separate sections: those in which orthophosphoric acid was used as the phosphorus source, and those in which phosphorus pentoxide was used.

Studies Using Orthophosphoric Acid as the Phosphorus Source. (a) Initial Energy Dispersive X-ray Diffraction (EDXRD) Studies. Initial studies using orthophosphoric acid as the phosphorus source were performed using the reaction composition $1Ga_2O_3$:$1P_2O_5$:2HF:1DAH:80H$_2$O, the composition used in laboratory syntheses.[17] Hereafter this composition will be referred to as the "standard" reaction composition. The course of a typical reaction performed at 180 °C is shown as a stack plot in Figure 3, which displays successive EDXRD patterns obtained during the synthesis of ULM-5 at 180 °C. After a short induction time of approximately 11 min in which no diffraction peaks are seen, diffraction peaks corresponding to the Bragg reflections of ULM-5 appear and grow in intensity, indicating the crystallization of the ULM-5 final product. The main point of note is the *extremely* rapid nature of the crystallization once it has begun. The acquisition time used in this reaction was just 30 s, yet within two spectra the product peaks have almost reached their maximum intensity. Extraction of the integrated intensities of the diffraction peaks for each 30 s spectrum was performed using an automated Gaussian fitting routine,[28] and yielded the data shown in Figure 4, which plots the intensities of the (011) and (002) reflections (the two intense reflections at ca. 40 and 47 keV) as a function of time.

(18) Giessen, B. C.; Gordon, G. E. *Science* **1968**, *159*, 973.
(19) Clark, S. M.; Miller, M. C. *Rev. Sci. Instrum.* **1990**, *61*, 2253−2255.
(20) Clark, S. M. *Rev. Sci. Instrum.* **1992**, *63*, 1010−1012.
(21) Clark, S. M.; Nield, A.; Rathbone, T.; Flaherty, J.; Tang, C. C.; Evans, J. S. O.; Francis, R. J.; O'Hare, D. *Nucl. Instrum. Methods, B* **1995**, *97*, 98−101.
(22) Clark, S. M.; Cernik, R. J.; Grant, A.; York, S.; Atkinson, P. A.; Gallagher, A.; Stokes, D. G.; Gregory, S. R.; Harris, N.; Smith, W.; Hancock, M.; Miller, M. C.; Ackroyd, K.; Francis, R.; O'Hare, D. *Mater. Sci. Forum* **1996**, *228−231*, 213-217.
(23) Norby, P. *Mater. Sci. Forum* **1996**, *228*, 147−152.
(24) Gualtieri, A.; Norby, P.; Hanson, J.; Hriljac, J. *J. Appl. Crystallogr.* **1996**, *29*, 707−713.
(25) Norby, P. *J. Appl. Crystallogr.* **1997**, *30*, 21−30.
(26) Norby, P. *J. Am. Chem. Soc.* **1997**, *119*, 5215−5221.
(27) Francis, R. J.; Price, S. J.; O'Brien, S.; Fogg, A. M.; O'Hare, D.; Loiseau, T.; Ferey, G. *Chem. Commun.* **1997**, 521.
(28) Clark, S. M. *J. Appl. Crystallogr.* **1995**, *28*, 646−649.

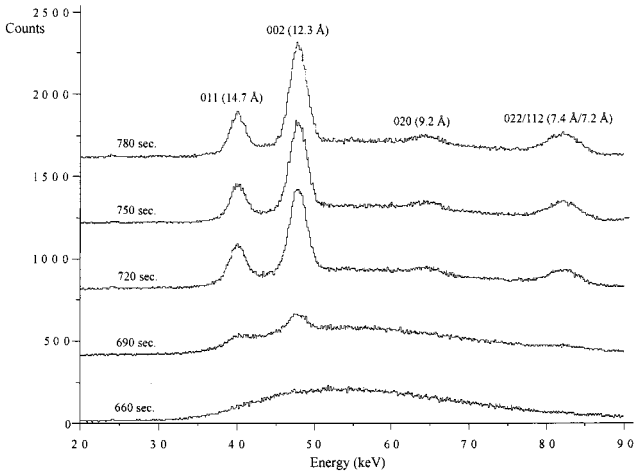

Figure 3. Stack plot of several individual EDXRD spectra showing the formation of ULM-5 at 180 °C.

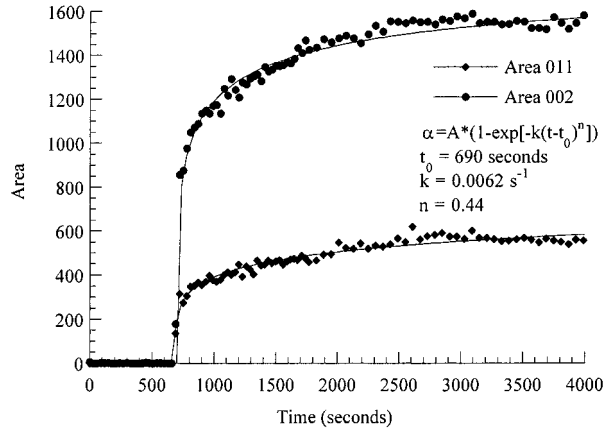

Figure 4. Growth in area with time of the (011) and (002) reflections of ULM-5 synthesized at 180 °C using orthophosphoric acid. Also shown are the calculated fits of the Avrami−Erofe'ev equation to the data, and the refined least squares parameters for the (002) reflection.

Three important conclusions can be reached by studying the data shown in Figure 4. First, the data emphasize the extremely rapid kinetics of the crystallization. The half-life of crystallization is less than 1 min (taking into account the induction time), and the reaction is essentially over approximately 50 min after the cell is introduced to the block. It is perhaps worth noting at this point that hydrothermal syntheses in the laboratory are typically performed over a time period of several *days*, rather than minutes. (ULM-5 itself is typically synthesized in the laboratory by reaction for a day.) The second point to note is that the data indicate that under these conditions the ULM-5 final product crystallizes directly from the amorphous reaction mixture, and does not pass through any crystalline intermediates prior to formation. Third, the intensity data for the (011) and (002) reflections have virtually identical shapes, indicating that the crystal growth is isotropic, with crystallographic ordering taking place at the same rate in all directions. [For the other Bragg reflections the intensity data have much more scatter associated with them due to the inherent weakness of these peaks. For this reason these data are not plotted in Figure 2. However, the crystallization curves for these peaks also conform to the same basic shape.] This is in contrast to the crystallization of the open-framework tin sulfide TMA-SnS-1 in which strongly anisotropic growth is observed.[29] This is perhaps to be expected given the three-dimensional framework nature of the ULM-5 structure, as opposed to the layer structure of TMA-SnS-1.

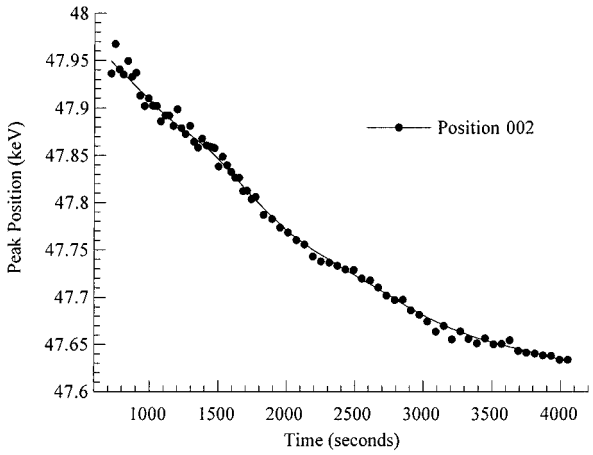

Figure 5. Shift in position of the (002) reflection of ULM-5 as a function of time.

Another interesting feature of the data obtained from this reaction is shown in Figure 5, which shows a plot of the position of the (002) reflection of ULM-5 with time. A slight but definite shift of the peak position to lower energies is seen as the reaction proceeds. This corresponds to a small (a change in energy of 0.3 keV is equivalent to a change in *d* spacing of ca. 0.1 Å at this angle) but significant shift to a higher *d* spacing. This feature is reproducible and is seen for other diffraction peaks in the spectra. Assuming this observation is not an artifact of the instrumentation or the data analysis procedure, which seems likely given that similar effects have not been seen in any other syntheses, this implies that the cell parameters of ULM-5 increase as the reaction proceeds. The explanation for this effect is not obvious, but one possibility is that the increase in the cell parameters is caused by an increase in the hydration level of the gallophosphate as the reaction proceeds. Such an effect has been observed previously in in situ studies of the formation of zeolitic materials.[26] The possibility that the increase in cell parameters is caused by a rise in the internal temperature of the cell was also considered. However, an increase of 0.1 Å in the cell parameters of ULM-5 due to an increase in temperature of, at most, 10 °C would imply a coefficient of expansion orders of magnitude higher than those seen in most materials.

(b) Kinetic Analysis. The study of the kinetics of solid-state reactions is useful in two respects. First, it enables one to obtain quantitative information (such as half-lives, rate constants, etc.) about the reactions and the factors affecting them, and second, it allows one to infer mechanistic information about the reactions studied. Many reviews of the area of solid-state kinetics have been published, both general[30−32] and more specific to hydrothermal reactions.[33] In general, kinetic analysis takes the form of fitting the experimental data to a theoretical expression relating the extent of reaction (α) and time. By making assumptions about the nucleation and growth processes, such as the number of dimensions in which growth occurs and the relative importance of nucleation and diffusion as the reaction proceeds, it is possible to derive specific forms of $f(\alpha)$ for a variety of possible mechanistic scenarios. Kinetic expressions

(29) Francis, R. J.; Price, S. J.; Evans, J. S. O.; O'Brien, S.; O'Hare, D.; Clark, S. M. *Chem. Mater.* **1996**, *8*, 2102−2108.
(30) Bamford, C. H.; Tipper, C. H. P. Theory of Solid State Reaction Kinetics. *Comprehensive Chemical Kinetics*; Elsevier Scientific Publishing Co.: New York, 1980; Vol. 22.
(31) Garner, W. E. *Chemistry of the Solid State*; Butterworth: London, 1955.
(32) Young, D. A. *Decomposition of Solids*; Pergammon Press: Oxford, 1966.
(33) Thompson, R. W.; Dyer, A. *Zeolites* **1985**, *5*, 202−210.

Table 1. Functional Forms of the Common Rate Equations Used To Model Solid-State Reactions

growth model	equation	label[a]	*n*
	Acceleratory Rate		
power law	$\alpha^{1/n} = kt$	P	*n*
	Sigmoidal Rate		
Avrami−Erofe'ev			
first order	$[\ln(1-\alpha)] = kt$	A1	1
second order	$[\ln(1-\alpha)]^{1/2} = kt$	A2	2
third order	$[\ln(1-\alpha)]^{1/3} = kt$	A3	3
fourth order	$[\ln(1-\alpha)]^{1/4} = kt$	A4	4
Prout−Tomkins	$\ln[\alpha/(1-\alpha)] = kt$		
	Deceleratory Rate		
1-D diffusion	$\alpha^2 = kt$	D1	0.62
2-D diffusion	$(1-\alpha)\ln(1-\alpha) + \alpha = kt$	D2	
3-D diffusion	$[1-(1-\alpha)^{1/3}]^2 = kt$	D3	0.57
Ginstling−Brounshtein	$1 - 2\alpha/3 - (1-\alpha)^{2/3} = kt$		
contracting area	$1-(1-\alpha)^{1/2} = kt$	C1	1.04
contracting volume	$1-(1-\alpha)^{1/3} = kt$	C2	1.08

[a] The labeling scheme applies to Figure 6.

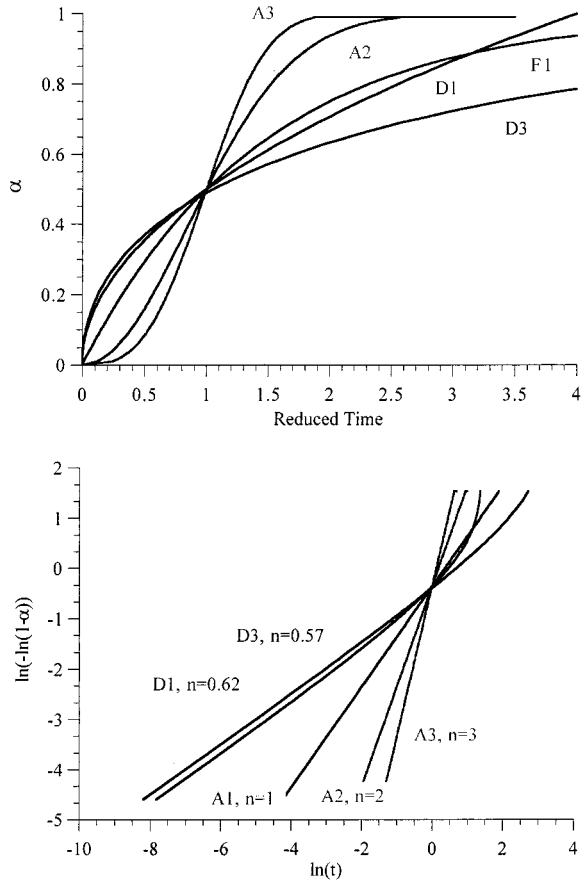

Figure 6. (a, top) Theoretical α vs time curves calculated for various models of crystal growth. (b, bottom) Sharp−Hancock plots calculated for various theoretical models of crystal growth.

that have found application in solid-state kinetics are detailed in Table 1, and the general shape of the crystallization curves for some of these models is shown in Figure 6a.

Initial kinetic analysis therefore usually involves comparison of the experimental data with the calculated curves for the theoretical models. However, a more rigorous approach involves the use of a Sharp−Hancock plot,[34] which is of the form

$$\ln[-\ln(1-\alpha)] = n\ln(t - t_0) + n\ln(k) \qquad (1)$$

where t is the time of reaction, t_0 is an optional term used to take into account any induction time or zero error, and k is the rate constant for the reaction. For all models of crystal growth listed in Table 1 the Sharp−Hancock plot is linear over the bulk of the reaction (ca. $\alpha < 0.1$ and $\alpha > 0.8$) with a gradient equal to the value of the exponent, n, and an intercept equal to $n\ln(k)$ (see Figure 6b). Therefore, testing the linearity of a Sharp−Hancock plot is a good way of determining if a reaction proceeds via a consistent mechanism, and since each of the theoretical models has a characteristic value of the exponent, n, the values of n extracted from such plots can be used to infer information about the mechanism of crystallization. The values of n for each of the theoretical models are also given in Table 1.

Initial analysis of the kinetic curves was performed by fitting the intensity data to the Avrami−Erofe'ev equation[35−38] using a least-squares algorithm. Typical fits for the (111) and (002) reflections of ULM-5 are shown in Figure 4 for a reaction performed at 180 °C, together with the values obtained for the induction time, rate constant, and reaction exponent, n, for the (002) reflection. Immediately apparent is the excellent fit that can be achieved over the entire range, and the very low value of the exponent for the reaction, which is a reflection of the rapidity of the increase in the intensity of the diffraction peaks during the early stage of the reaction. The values obtained in this way were reproducible, with a number of reactions performed under identical conditions consistently yielding values of n in the range 0.44−0.50.

The validity of this fit was confirmed via a Sharp−Hancock analysis of the kinetic data. Although some deviations were seen in the very early and late stages of the reaction, over the vast majority of the reaction ($0.1 < \alpha < 0.9$), the plot of $\ln[-\ln(1-\alpha)]$ vs $\ln(t - t_0)$ is linear, indicating that the crystallization proceeds via a consistent mechanism over almost the entire course of the reaction. Furthermore, the Sharp−Hancock plot confirms the value of the exponent obtained above, yielding a value of 0.47 ± 0.02.

The very low value for the exponent and the very rapid initial increase in the diffraction intensity both strongly suggest that the crystallization of ULM-5 under these conditions is a diffusion-controlled process. To test this hypothesis, the function $[1-(1-\alpha)^{1/3}]^2$ was plotted against $(t - t_0)$. For a diffusion-controlled process in three dimensions such a plot should result in a straight line with gradient k (see Table 1). The plot is shown in Figure 7, and it can be seen that the plot is indeed linear over virtually the entire course of the reaction, although some small deviations from linearity were seen at low and high values of α. Other possible models of the growth process were also tested by plotting the appropriate functional forms of α against t (Table 1). All of these models produced markedly nonlinear plots.

We therefore conclude that under these experimental conditions the synthesis of ULM-5 is consistent with a *purely diffusion-controlled process* in which the rate of nucleation does not play a role in determining the rate of reaction once crystallization has begun. Thus, the crystallization can be likened to the crystallization of a supersaturated solution, in which once nucleation has occurred, the rate of crystallization is determined only by the rate at which species in solution can diffuse onto the nucleation site. The extremely rapid rates seen in these reactions is probably a consequence of the fact that these

(34) Hancock, J. D.; Sharp, J. H. *J. Am. Ceram. Soc.* **1972**, *55*, 74−77.
(35) Avrami, M. *J. Chem. Phys.* **1939**, *7*, 1103.
(36) Avrami, M. *J. Chem. Phys.* **1940**, *8*, 212.
(37) Avrami, M. *J. Chem. Phys.* **1941**, *9*, 177.
(38) Erofe'ev, B. V. *C. R. Dokl. Acad. Sci. URSS* **1946**, *52*, 511.

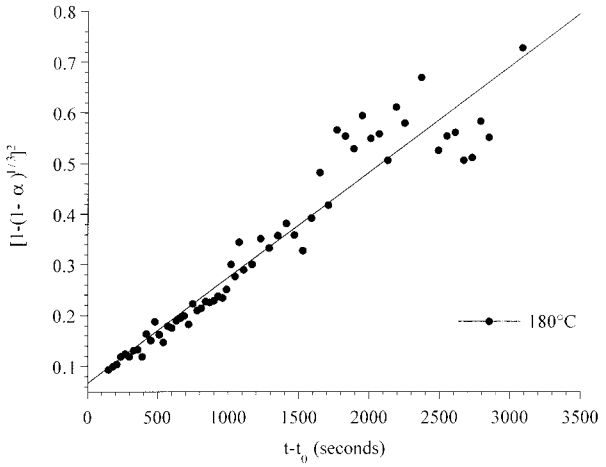

Figure 7. $[1 - (1 - \alpha)^{1/3}]^2$ against time for the growth of the (002) reflection of ULM-5 at 180 °C.

reactions are being stirred fairly vigorously, which clearly will have the effect of greatly increasing the rate at which species are transported to the nucleation sites relative to a simple diffusion process (vide infra).

(c) Variable Temperature Studies. To assess the effect of temperature on the crystallization of ULM-5, reactions were performed using the standard reaction composition at temperatures in the range 140−180 °C. Sharp−Hancock analysis of the data showed that over this temperature range the reactions obeyed kinetics very similar to those of the reaction discussed above, yielding values for the exponent in the range 0.45 ± 0.04 for all temperatures studied (see Table 2).

Table 2. Values of the Induction Times, Exponents, and Rate Constants Obtained from Plots of $\ln[-\ln(1 - \alpha)]$ vs $\ln(t - t_0)$ for Reactions Carried out at Five Different Temperatures

temp (±1 °C)	induction time (s)	$n_{(011)}$	$n_{(002)}$	rate constant[a] (s^{-1})
180	720	0.44(3)	0.49(3)	$5.7(5) \times 10^{-3}$
170	900	0.46(3)	0.49(2)	$5.4(2) \times 10^{-3}$
160	2600	0.43(3)	0.49(3)	$5.8(4) \times 10^{-3}$
150	1050	0.43(2)	0.43(2)	$12.3(4) \times 10^{-3}$
140	4200	0.41(2)	0.41(2)	$18.0(5) \times 10^{-3}$

[a] Average value obtained from fitting of both (011) and (002) reflections.

The similar exponent values suggested that the reactions conform to the same general mechanism as the reaction at 180 °C over the entire temperature range. Plots of $[1 - (1 - \alpha)^{1/3}]^2$ against t for all of the reactions confirmed that the three-dimensional diffusion model of crystal growth was the most valid model of the crystal growth process for each of the reactions studied, although some deviations from linearity were observed at low values of α, indicating that diffusion-limited kinetics do not accurately describe the reaction kinetics at very early times in the crystallization. This reflects the rather lower values of n than would be expected for diffusion-controlled kinetics in some of the reactions studied. Figure 8 shows the plot of $[1 - (1 - \alpha)^{1/3}]^2$ against t for the reactions performed at 150, 160, 170, and 180 °C.

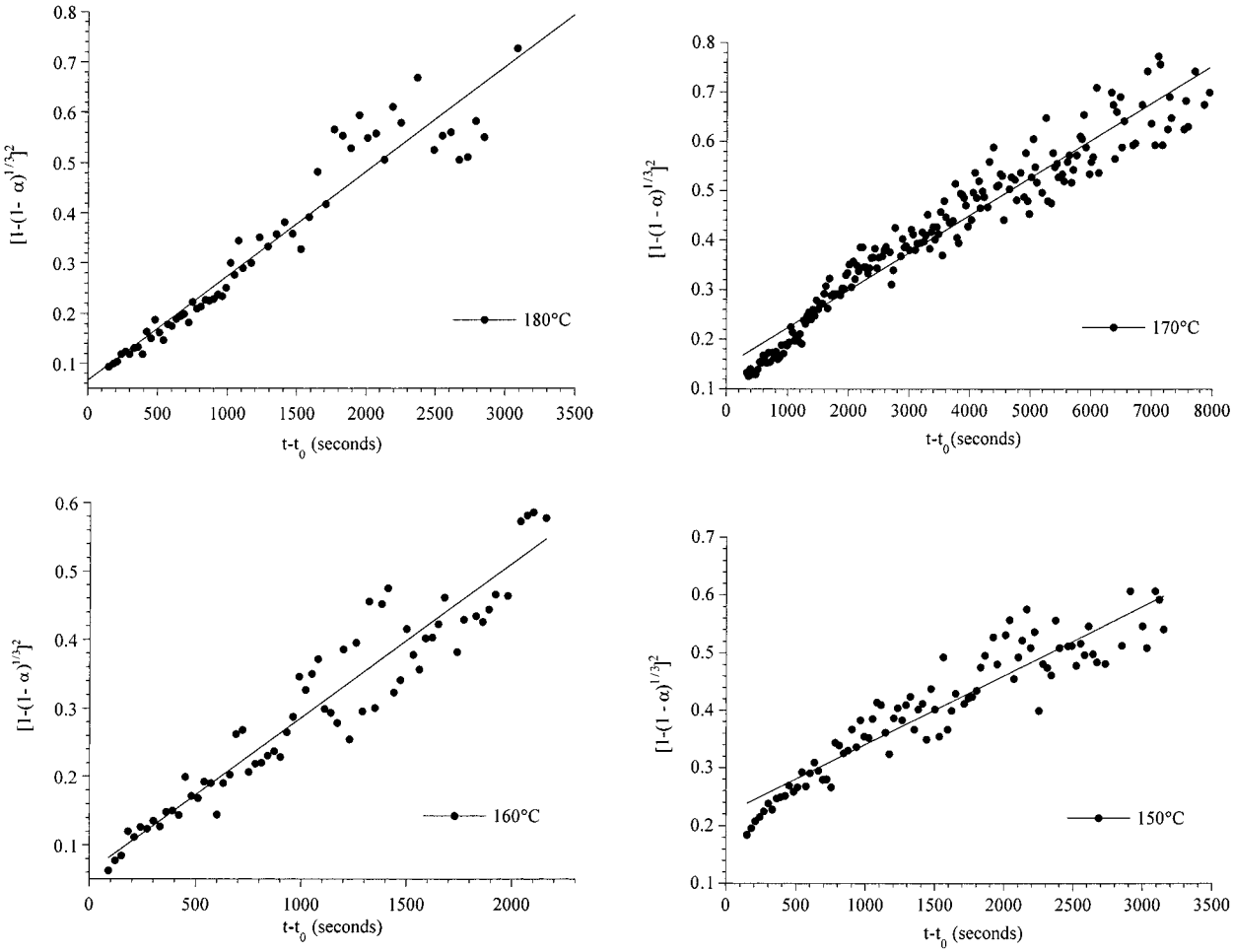

Figure 8. $[1 - (1 - \alpha)^{1/3}]^2$ against time for the growth of the (002) reflection of ULM-5 at (a, top left) 180 °C, (b, top right) 170 °C, (c, bottom left) 160 °C, and (d, bottom right) 150 °C.

Table 3. Values of the Induction Times, Exponents, and Rate Constants Obtained from Plots of $\ln[-\ln(1-\alpha)]$ vs $\ln(t-t_0)$ for Reactions Carried out at Five Different Water Stoichiometries

stoichiometry Ga_2O_3:H_2O	induction time (s)	$n_{(011)}$	$n_{(002)}$	rate constant[a] (s^{-1})
1:1	720	0.44(3)	0.49(3)	$5.7(5) \times 10^{-3}$
1:2	1200	0.50(2)	0.60(2)	$9.6(4) \times 10^{-3}$
1:3	1020	0.46(5)	0.45(5)	$3.3(8) \times 10^{-3}$
1:4	1020	0.57(2)	0.58(2)	$4.0(2) \times 10^{-3}$

[a] Average value obtained from fitting of both (011) and (002) reflections.

Rate constants for the reactions can be easily extracted from Sharp−Hancock plots, since the value of the intercept is equal to $n \ln(k)$. The values obtained in this way for each temperature studied are listed in Table 2. It can be seen that there are no clear trends in the value of the rate constant with respect to temperature. [Although the values given in Table 2 seem to indicate that there is some correlation of the rate constant with temperature, it should be noted that the rate constants obtained from these experiments are not highly reproducible. The values listed in Table 2 were obtained from analysis of the data shown in Figure 8. Analysis of many other experiments performed at various temperatures indicates that there is no correlation of rate constant with temperature.] This observation reflects the fact that for a diffusion-controlled reaction the rate of crystallization is determined by how quickly species are transported to the growth centers. Under these experimental conditions this rate may depend primarily on how vigorously the reaction mixtures are being mechanically stirred rather than the inherent rate of diffusion under static conditions. Therefore, the differences in observed reaction rate may reflect small differences in stirring rate used in each of the experiments. Also listed in Table 2 are the values for the induction times observed at each temperature. Although there is a general trend to longer induction times with decreasing temperature, the trend is not smooth and there are anomalies (notably the 150 °C reaction). In addition, the induction times were not reproducible and reactions performed at the same temperature several times yielded different values for the induction period each time. The values given in Table 2 should therefore only be taken as a guide to the kind of values observed in these experiments.

(d) Variable pH Studies. The effect of pH on the kinetics of the synthesis of ULM-5 was studied in two ways. In the first, reaction compositions of $1Ga_2O_3$:xP_2O_5:1HF:1DAH:$80H_2O$, where $x = 1$, 1.5, and 2.5, were reacted at 180 °C; i.e., the quantity of orthophosphoric acid was increased above that used in the standard reaction composition. In the second, reaction compositions of $1Ga_2O_3$:$1P_2O_5$:1HF:1DAH:xH_2O, where $x =$ 80, 160, 240, and 320, were reacted at 180 °C; i.e., the quantity of water was increased over the standard reaction composition, raising the reaction pH.

In the first case, as the pH was decreased, it was found that an increasing quantity of condensed $GaPO_4$ was formed in addition to ULM-5. At a P_2O_5 stoichiometry of $x = 2.5$, $GaPO_4$ was the only product observed in the reaction. At a stoichiometry of $x = 1.5$, a mixture of ULM-5 and $GaPO_4$ was formed in the reaction. The kinetics of formation of ULM-5 were found to be identical to those performed under standard reaction conditions.

In the second case, it was found that at each of the stoichiometries studied the reactions displayed kinetic behavior similar to that of the reactions studied previously. Avarmi−Erofe'ev and Sharp−Hancock analysis of the data yielded values for the exponent in the range 0.45−0.57 (see Table 3), i.e., somewhat higher than the values that had been observed previously, but still well within the expected range for a diffusion-controlled three-dimensional growth mechanism. Plots of $[1-(1-\alpha)^{1/3}]^2$ against t (shown in Figure 9) showed excellent linearity for all four reactions, confirming the validity of this growth model. The values for the rate constants and induction times for each stoichiometry again showed no clear trends. Table 3 lists the values of the exponents, induction times, and rate constants for each reaction.

(e) Discussion. The observation of diffusion-controlled kinetics in the hydrothermal synthesis of ULM-5 is remarkable given the complexity of the structure of ULM-5. It is also unprecedented within the field of molecular sieve syntheses. In most syntheses of molecular sieves studied to date, either acceleratory kinetics are observed in which the rate of product growth increases with time,[39−42] or Avrami−Erofe'ev type nucleation and growth kinetics with orders in the range 1.0−4.0 are observed.[26,43] To our knowledge, this is the first known example of diffusion-controlled kinetics being observed in the synthesis of molecular sieve materials.

In those systems in which acceleratory kinetics have been observed, such as the syntheses of zeolites A and X,[41,42] such kinetics have been attributed to an autocatalytic nucleation mechanism in which the majority of nucleation centers are formed within the gel, and are therefore "hidden" from the liquid phase and cannot grow until they are released from the gel as it dissolves during crystallization. Hence, as the crystallization proceeds, the number of nucleation centers increases, the rate of crystallization increases, further nucleation centers are released, and the rate continuously increases until crystallization is complete. Such kinetics are therefore only observed in markedly inhomogeneous systems consisting of distinct solid and liquid phases. The observation of diffusion-controlled kinetics in the synthesis of ULM-5 under these conditions implies that the crystallization takes place from a much more homogeneous reaction medium than those in which acceleratory kinetics are observed.

On the basis of observations of the close structural relationships between several of the gallophosphate members of the ULM-*n* family, and in particular the existence of several phases that can be synthesized in the same systems under different conditions, Férey has proposed a mechanism of formation of the ULM-*n* materials in which the final crystalline products are formed via the condensation of solution-phase oligomeric secondary building units (SBUs).[15,16] These SBUs are envisioned to grow until their size, shape, and charge density match those of the template used. At this point it is postulated that a strong template−SBU association is formed which is electronically neutral and can be compared to a cation−anion pair. An infinite condensation of these template−SBU associations is then envisioned to occur to form the final framework material.

The observation of diffusion-controlled kinetics is consistent with such a process in which prior to the onset of crystallization the required "building blocks" for the formation of the final crystalline product are already present throughout a homogeneous reaction mixture. The observed kinetics are also consistent with a solution-phase process in which very rapid kinetics could be expected, assuming that once crystallization has begun the condensation of the building blocks into the growing crystallites

(39) Zhdanov, S. P. *Adv. Chem. Ser.* **1971**, *101*, 20.
(40) Kacirek, H. *J. Phys. Chem.* **1976**, *80*, 1291−1296.
(41) Subotic, B. *ACS Symp. Ser.* **1989**, *398*, 110−123.
(42) Antonic, T.; Subotic, B.; Stubicar, N. *Zeolites* **1997**, *18*, 291−300.
(43) Di Renzo, F.; Remoue, F.; Massiani, P.; Fajula, F.; Figueras, F.; Descourieres, T. *Zeolites* **1991**, *11*, 539−548.

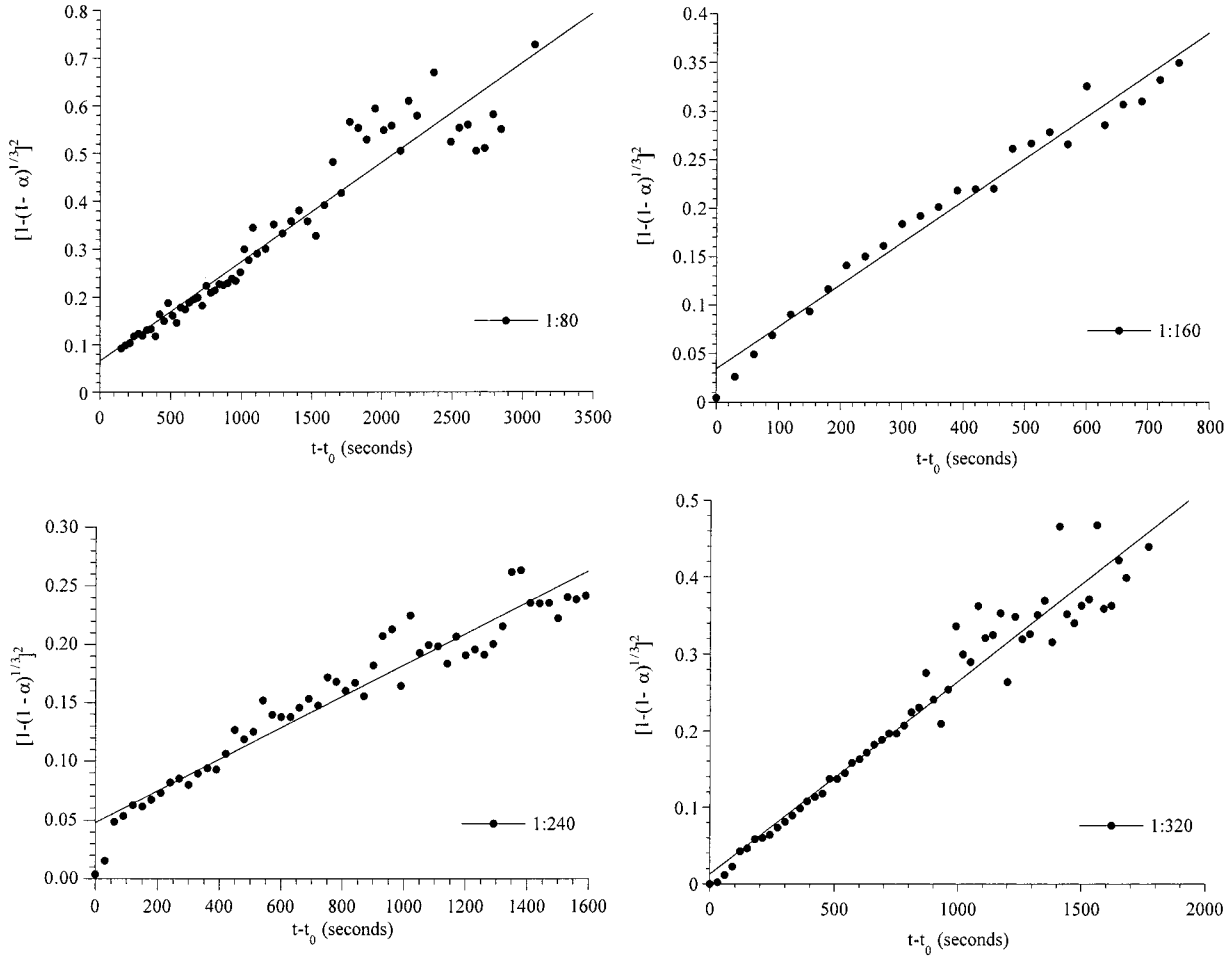

Figure 9. $[1 - (1 - \alpha)]^{1/3}]^2$ against time for the growth of the (002) reflection of ULM-5 using a Ga_2O_3:H_2O ratio of (a, top left) 1:80, (b, top right) 1:160, (c, bottom left) 1:240, and (d, bottom right) 1:320.

is an extremely facile process. It is also notable that in recent in situ EDXRD studies which we have performed on the syntheses of other members of the ULM-*n* family, such as ULM-3 and ULM-4,[44] crystallization kinetics similar to those described above are observed, which would be expected if these materials are all synthesized via a similar mechanistic process. However, it must be emphasized that although the observed kinetics are consistent with such a process, they do not provide direct evidence for, or provide any information about the structures of, any postulated SBUs in solution. In situ NMR and in situ EXAFS experiments on the hydrothermal synthesis of ULM-5 are currently underway with a view to determining the existence and structures of any species in solution during the syntheses of these materials.

Studies Using Phosphorus Pentoxide as the Phosphorus Source. (a) Initial in Situ EDXRD Studies. When the synthesis of ULM-5 is performed using the standard reaction composition ($1Ga_2O_3$:$1P_2O_5$:2HF:1DAH:$80H_2O$), but with phosphorus pentoxide replacing orthophosphoric acid as the phosphorus source, dramatically different behavior is observed. The time evolution of the EDXRD pattern during the synthesis of ULM-5 at 180 °C under these conditions is shown as a three-dimensional plot in Figure 10. After a short induction time of ca. 4 min, diffraction peaks due to a previously unknown highly crystalline intermediate appear which grow rapidly in intensity, reaching a maximum after ca. 18 min. After this point, these peaks immediately begin to decrease in intensity and peaks due to ULM-5 begin to appear and grow in intensity. The decay of the diffraction peaks is much slower than their initial growth, taking over 70 min for the peaks to completely disappear. At this point, the ULM-5 peaks reach maximum intensity and there is no further change in the diffraction pattern. Figure 10 shows the growth and decay of the peaks due to the intermediate phase, and the growth of the peaks due to the ULM-5 final product. Figure 11 shows a plot of the extracted intensities for the (002) reflection of ULM-5 and the intermediate reflection at 13.1 Å. From Figure 11, the high degree of correlation between the decay of the intermediate peak and the growth of the product

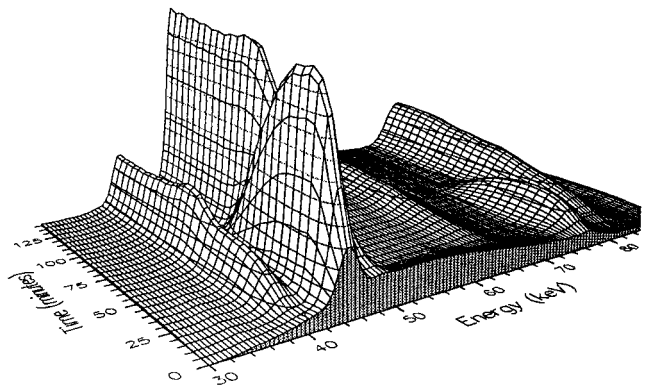

Figure 10. Three-dimensional plot of the evolution of the energy dispersive diffraction pattern with time during the synthesis of ULM-5 at 180 °C using phosphorus pentoxide as a starting material. The acquisition time for each spectrum was 60 s at a diffraction angle of 1.25°.

(44) Francis, R. J.; Walton, R. I.; Loiseau, T.; O'Hare, D. Unpublished results.

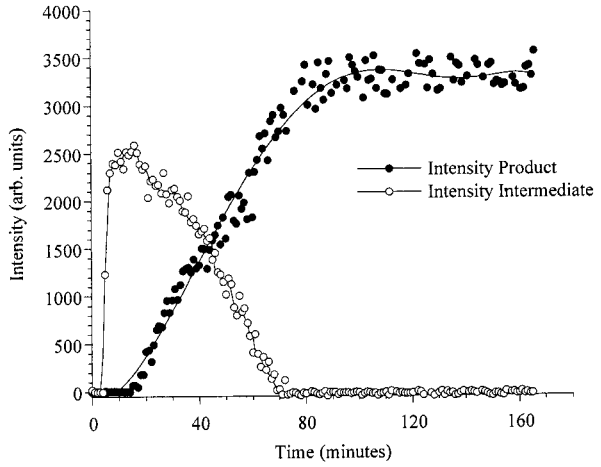

Figure 11. Variation of intensity with time of the (002) reflection of ULM-5 (filled circles) and the 13.1 Å peak of an intermediate crystalline phase (open circles) during the synthesis of ULM-5 at 180 °C using phosphorus pentoxide as a starting material.

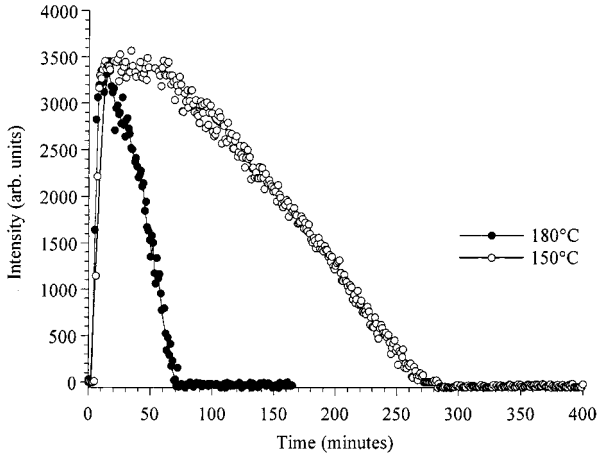

Figure 12. Comparison of the variation with time of the 13.1 Å reflection of the intermediate phase at 180 °C (filled circles) and 150 °C (open circles).

peak can be readily appreciated. This suggests that the two phases may be closely related, with the intermediate phases being directly converted into the final product.

The determination of the composition and the structure of this intermediate is clearly of importance and interest for its mechanistic implications in the formation of ULM-5. Therefore, experiments were performed to determine conditions in which the intermediate was relatively long-lived, with a view to performing quenching experiments to isolate the intermediate and attempt an ex situ structure determination. These experiments revealed that as the temperature is lowered the growth and decay of the intermediate peaks becomes slower, and the intermediate becomes increasingly long-lived. At 150 °C the beginnings of a "plateau" in the intensity of intermediate peaks could be seen during which the intensity of the intermediate does not decrease and no peaks due to ULM-5 are seen. Figure 12 shows a comparison of the area of the intermediate peak with time for the reactions at 180 and 150 °C. As the temperature is lowered further to 130 °C, this plateau in intensity becomes pronounced and the intermediate is very long-lived. These results suggested the possibility of isolating a pure sample of the intermediate by quenching the reaction after the intermediate peaks have reached maximum intensity.

Therefore, experiments were performed in which the reactions were monitored in real time using the in situ EDXRD facility, and once the intermediate peaks were observed to reach maximum intensity, the cell was removed from the block and quenched with cold water. Unfortunately, successful isolation of a sample of the intermediate using this protocol proved to be difficult. The quenching experiment was repeated many times, and in only two instances did it prove possible to isolate a phase with a powder X-ray diffraction pattern which matched that seen in the energy dispersive spectrum immediately prior to quenching, indicating that the intermediate phase is very sensitive to the quenching and workup procedure. The samples that matched the X-ray pattern seen in the energy dispersive spectra also proved to be metastable, and transformed over a period of days to another as yet unidentified phase, frustrating attempts to obtain a high-resolution X-ray diffraction pattern of the material suitable for structural analysis. Attempts to index this phase on the basis of the relatively low-resolution data obtained before the transformation had occurred did not produce any convincing cells, although the powder X-ray data did reveal the presence of unreacted gallium oxide and gallium hydroxyoxide (GaO(OH)) in the quenched material. Attempts to index the "workup transformed" or phase produced via transformation of the isolated intermediate phases using high-resolution XRD data were similarly unsuccessful.

Owing to the sensitivity of the intermediate phase to quenching and workup, there seemed to be little possibility of a successful ex situ structure determination. Therefore, attempts were made to obtain data suitable for structural analysis in situ. However, the low-resolution data obtained using energy dispersive diffraction are not suitable for structure solution or refinement. Therefore, in an effort to gain a greater understanding of the structural relationships between these phases, we undertook an in situ angular dispersive study of the synthesis of ULM-5 using monochromatic synchrotron X-ray radiation. In principle the quality of the high-resolution data obtainable using such a system should allow the determination of the structure of any intermediate phases via ab initio solution methods.

(b) In Situ Angular Dispersive X-ray Diffraction (ADXRD) Experiments. These were performed on the ULM-5 system by syringing aliquots of the reaction mixture into capillaries and heating at 160 °C for 3 h. Figure 13 shows three-dimensional plots of the evolution with time of the powder diffraction patterns for three experiments performed in this manner. As can be seen from the figure, these experiments revealed much more complex behavior than was seen in the experiments performed at Daresbury. Despite being prepared in an identical manner, each of the three experiments displayed completely different behavior. Although in each case the final product formed was ULM-5 as expected, the time taken for completion of the reaction was markedly different in each case. More dramatically, the diffraction patterns of the intermediate were completely different in each case. Differences were seen throughout the powder diffraction patterns, but the most obvious differences centered around the intermediate peaks at 13.1 and 12.2 Å. The first experiment, shown in Figure 13a, showed behavior similar to that observed at Daresbury, with the most intense peak due to the intermediate phase at 13.1 Å, a smaller peak at 12.2 Å, and other small peaks. However, in the second experiment, shown in Figure 13b, the peak at 12.2 Å is completely absent. By contrast, in the third experiment, shown in Figure 13c, the peak at 13.1 Å is completely absent, and the peak at 12.2 Å is the most intense peak in the spectrum.

We therefore conclude that, when phosphorus pentoxide is used as a starting material, ULM-5 can be formed via *two*

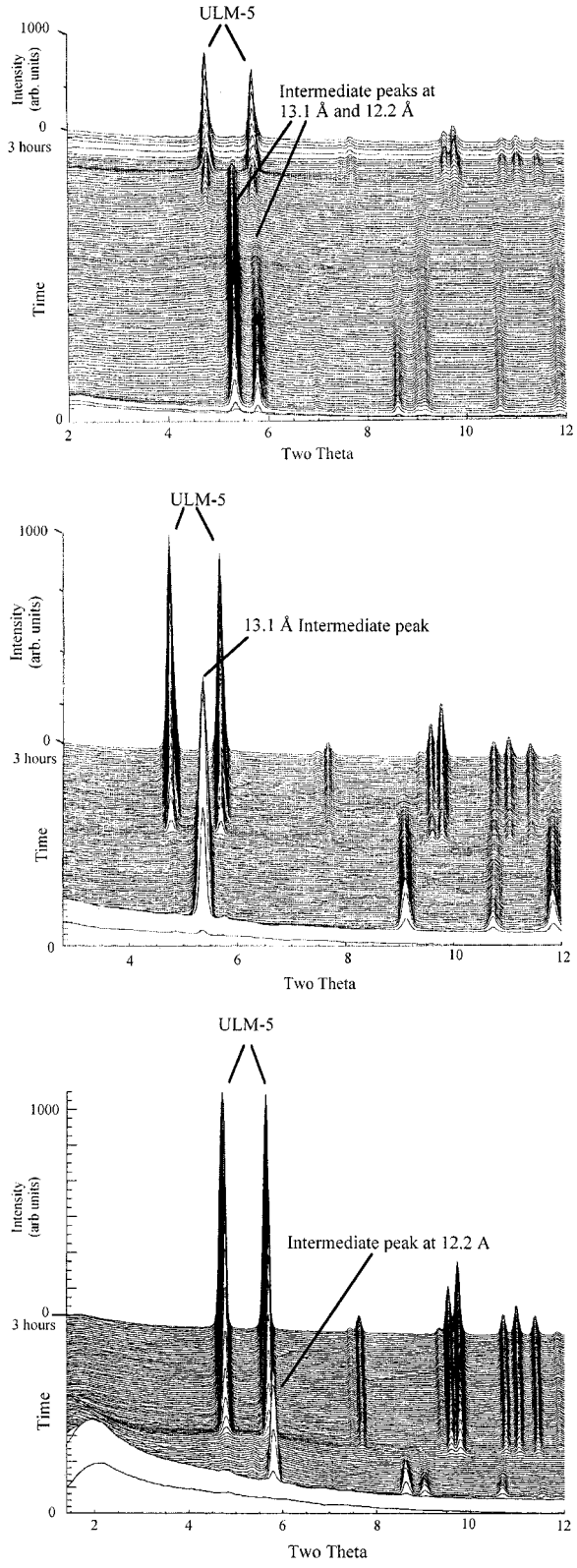

Figure 13. (a, top) Evolution with time of the angular dispersive X-ray diffraction pattern during the synthesis of ULM-5 using phosphorus pentoxide, showing the formation of reflections due to the intermediate phase at 13.1 and 12.2 Å. (b, middle) Evolution with time of the angular dispersive X-ray diffraction pattern during the synthesis of ULM-5 using phosphorus pentoxide, showing the formation of a reflection due to the intermediate phase at 13.1 Å, but no reflection at 12.2 Å. (c, bottom) Evolution with time of the angular dispersive X-ray diffraction pattern during the synthesis of ULM-5 using phosphorus pentoxide, showing the formation of a reflection due to the intermediate phase at 12.2 Å, but no reflection at 13.1 Å.

completely different crystalline intermediate phases. Hereafter these two phases will be referred to as intermediates I and II. In any particular experiment the ULM-5 final product may be formed via one or other of the two intermediate phases exclusively, or a mixture of both phases, situations exemplified by parts b, c, and a, respectively, of Figure 13. It must also be concluded that the experiments performed at Daresbury resulted in the formation of a mixture of intermediate phases, which may partially account for the failure to index any of the products recovered from the quenching experiments.

Individual powder X-ray patterns were extracted from the data at the time of maximum intensity of the intermediate phases in each of the three cases. In this way individual spectra of both intermediate phases could be obtained, as well as a spectrum of the mixture of phases. Attempts were made to index both intermediate phases using the auto-indexing programs TREOR90[45] and ITO.[46] These resulted in a variety of possible cells for the two phases. However, the figures of merit obtained were fairly low, and none of the cells were entirely convincing. We now believe that the previously reported cells for the intermediate phases may be in error.[27]

Comment should be made as to why, given that each of the three experiments described above was performed in exactly the same manner, such dramatically different behavior was seen in each case, and why much more consistent behavior was seen in the experiments performed at Daresbury. This appears to be a case in which the difficulty of reproducing precisely the same reaction conditions numerous times using small-volume capillaries becomes important. This particular reaction appears to suffer particularly from irreproducibility, due to both the sensitivity of the reaction pathway to small changes in the reaction conditions and the inhomogeneous nature of the reaction mixture. After the reagents are mixed in the appropriate quantities, the reaction mixture consists of both solid and liquid phases. It was found to be impossible to prepare capillaries which contained precisely the same amounts of solid and liquid phases each time. It seems likely that it is these unavoidable changes in the ratios of the various reaction components that is the cause of the irreproducible nature of the reactions. When using the large-volume cell for EDXRD studies, such problems do not arise because in each case the complete sample mixture is contained within the reaction cell and the ratio of components is always precisely known.

(c) Further in Situ Studies Using EDXRD. To test this hypothesis, further experiments were performed at Daresbury using the large-volume reaction cell in which the ratios of the various reaction components were systematically varied. The quantities of four of the starting reagents, Ga_2O_3, P_2O_5, HF, and DAH, were separately increased or decreased from the standard reaction composition, and the effect on the reaction pathway was monitored using time-resolved EDXRD.

Variation of the quantity of Ga_2O_3 yielded inconclusive results. However, variation of the quantity of P_2O_5 was found to have a dramatic effect on the reaction pathway. Increasing the P_2O_5 ratio by just 10% was found to result in the formation of purely intermediate phase I, whereas decreasing the ratio by 10% was found to result in the formation of purely intermediate phase II. Figure 14 illustrates the results of these experiments and highlights the differences. These results are reproducible. Similar results were obtained from those experiments in which the quantities of HF and DAH were varied. Increasing the

(45) Werner, P. E.; Eriksson, L.; Westdahl, M. *J. Appl. Crystallogr.* **1985**, *18*, 367−370.
(46) Visser, J. W. *J. Appl. Crystallogr.* **1969**, *2*, 89.

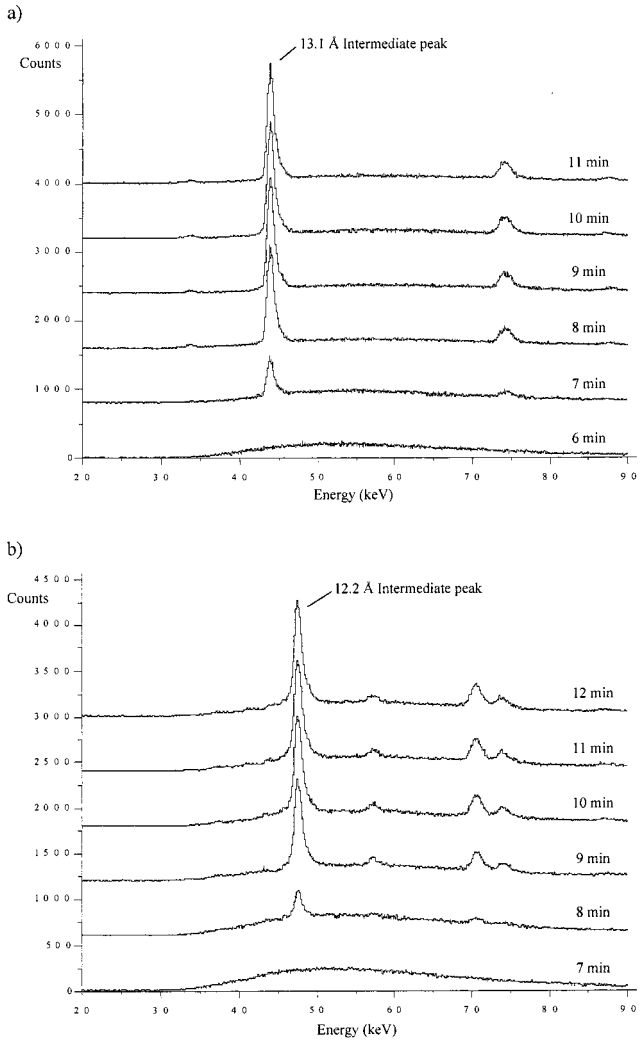

Figure 14. Stack plots of the evolution with time of the EDXRD patterns recorded during the synthesis of ULM-5 using (a) 1.1 times the standard quantity of P_2O_5 and (b) 0.9 times the standard quantity of P_2O_5 showing (a) the formation of exclusively intermediate phase I and (b) the formation of exclusively intermediate phase II.

Table 4. Effect of Changing the Reaction Stoichiometry on the Intermediate Phases Formed during the Synthesis of ULM-5 Using P_2O_5

reactant stoichiometry					intermediate phase formed
Ga_2O_3	P_2O_5	HF	1,6-DAH	H_2O	
1	1	2	1	80	I plus small quantity of II
1	1.1	2	1	80	I exclusively
1	1	2.3	1	80	I exclusively
1	1	2	0.85	80	I exclusively
1	0.9	2	1	80	II exclusively
1	1	1.7	1	80	II exclusively
1	1	1	1.15	80	II exclusively

quantity of HF by 15% or decreasing the quantity of DAH by 15% led to the formation of intermediate phase I exclusively, whereas decreasing the quantity of HF by 15% or increasing the quantity of DAH by 15% led to the formation of intermediate phase II exclusively (see Table 4). In some of these cases other previously unobserved phases were formed at longer reaction times after the conversion of the intermediate phases to ULM-5. Other reaction products are known to be formed in this system if the ratio of reagents is changed significantly (particularly DAH).[47] This does not affect the results of these experiments, however.

These results conclusively show that the relative quantities of the various reaction components do strongly influence the pathway followed by this reaction. A small increase of the relative quantity of P_2O_5 or HF or a decrease in the quantity of DAH favors the formation of intermediate phase I, while the reverse change favors intermediate II formation. It is notable that all of these results are consistent with regard to the change in pH of the reaction, with a lower pH composition favoring intermediate I, and a higher pH composition favoring intermediate II. Férey and co-workers suggest that the pH of solution affects the nature of species in solution in a number of ways, including (i) the degree of hydration of the template, (ii) the coordination of the gallium atom (from tetrahedral to trigonal bipyramidal to octahedral as the pH is lowered), and (iii) the size of the SBU polyhedra. Clearly, both intermediates are kinetic products, and at low pH the species in solution favor the formation of intermediate I, whereas at higher pH the species in solution are more conducive to intermediate II formation. It appears the standard reaction composition happens to lie at a point at which the factors favoring formation of one phase over the other are very finely balanced. This fact, coupled with the sampling difficulties discussed earlier, provides an explanation for the irreproducibility of the experiments performed at Brookhaven. In particular, the relative quantities of basic gallophosphate solid and the acidic liquid components introduced to the capillary are clearly going to have a strong effect on the pH of the reaction mixture, which these experiments suggest is an important factor in determining the reaction pathway. Although the experiments performed at Daresbury show much higher reproducibility, close scrutiny of the relative intensities of the 13.1 and 12.2 Å peaks in experiments performed using ostensibly the same reaction composition show some small differences. This perhaps reflects the difficulty of weighing P_2O_5 to a high degree of accuracy owing to its hydroscopic nature.

(d) Discussion. The observation of the formation, under certain reaction conditions, of two intermediate crystalline phases during the synthesis of ULM-5 is clearly of central importance for an understanding of the processes occurring during the formation of this material, and is of interest for the better understanding of hydrothermal reactions in general. There are three issues of particular importance: Do the intermediate phases convert directly into the product phase via a solid−solid transformation, or via some kind of solution-mediated process? Why does the form of the phosphorus source have such a dramatic effect on the reaction pathway? Why, when P_2O_5 is used, does the precise reaction composition also have such a major effect on the reaction, and what are the structures of the two intermediate phases?

Regarding the mechanism of transformation of the intermediates to the final product, there are four distinct possibilities: (1) a direct solid−solid transformation involving an internal rearrangement of the frameworks with no intermediate amorphous or solution phases involved in the process, (2) a process in which the intermediate phases are converted completely or partially into an amorphous phase from which the product phase subsequently nucleates and crystallizes, (3) a solution-mediated process in which complete dissolution of the intermediate phases occurs, followed by the nucleation and growth of the final product, (4) the formation of the intermediate and product phases as completely separate processes, in which the prior formation and decay of the intermediate phases is simply a reflection of the different kinetics of formation of the different phases, i.e.,

(47) Loiseau, T.; Ferey, G. Unpublished results.

the ULM-5 final product forms separately from the onset of crystallization, but at a much slower rate than the formation or decay of the intermediates.

Information about which one of these possibilities is likely to be the correct one can be gained from the crystallization and degradation curves for the various phases in the system. Figure 11 is a typical example of these data, and shows that the decay of the intensity of the intermediate phase (intermediate phase I in this case) is *very* highly correlated with the growth of the product phase, with the onset of decay occurring simultaneously with the onset of crystallization of the product, and finishing as the product peak reaches maximum intensity. This correlation is seen in reactions carried out over a wide range of reaction conditions, and thus, the possibility of the formation of intermediate and product being completely separate processes can be immediately ruled out. Additionally, the curves cross at very close to $\alpha = 0.5$, implying that the quantity of amorphous- or solution-phase species involved in the transformation is very small, since if significant quantities of the intermediate phase were dissolved or converted into an amorphous phase, the curves would be expected to cross well below $\alpha = 0.5$. The sum of the α values for the two phases remains close to 1 throughout the reaction, although it does rise to slightly greater than 1 during the early stages of the decay of the intermediate, before falling back to 1. This indicates that the rate of decay of diffraction peaks is slower than the rise in intensity of the product peaks, and may indicate that the formation of the intermediate continues after formation of the product has begun. Analysis of the fwhm of the reflections of the intermediate phase showed no broadening of the diffraction peaks with time, indicating that there is no significant loss in crystallinity of the intermediate phases as the reaction progresses, as would be expected if there was complete dissolution of the intermediate phase to form a solution or amorphous phase. [This analysis was performed on the data obtained at Brookhaven using angular dispersive diffraction. Similar analysis of the EDXRD data obtained at Daresbury is not informative, because, due to the inherently low resolution of the EDXRD technique, the peak widths are always determined by the inherent resolution of the technique and not the crystallinity of the sample, and therefore remain constant with time. This analysis relates to the behavior of intermediate phase I in a reaction in which there was also a small amount of intermediate phase II present. The transformation behavior is essentially identical in reactions in which only intermediate phase I is present, however. Analysis of the transformation kinetics of intermediate phase II is complicated by the presence of a Bragg reflection of ULM-5 at exactly the same *d* spacing as the intermediate reflection. However, it is clear that the transformation kinetics display the same general features as for intermediate phase I; i.e., the decay of intermediate phase II and the growth of ULM-5 are highly correlated.]

These results strongly indicate either that the mechanism of transformation is a direct solid−solid conversion involving no other amorphous or solution phases, or that if amorphous or solution phases are involved, the quantities of such phases present at any particular time are very small, and the transformation must only involve the dissolution of a small quantity of material at the surface of the intermediate crystallites. To fully distinguish between these two possibilities, other measurements using other in situ techniques are necessary. In this regard in situ NMR studies would be particularly informative because they would reveal the presence of any amorphous phases or solution species that appear in the reaction mixture during the period in which the intermediate(s) are undergoing the transformation to the final product. However, although such studies on this system are underway, no conclusive results are yet available. Intermediate phases have been observed by in situ NMR experiments during the formation of the aluminophosphate $AlPO_4$-CJ2[48,49] and the gallophosphates ULM-3 and ULM-4.[50] However, at this point it is not clear whether these intermediate phases are crystalline, and how these results may be related to the synthesis of ULM-5.

The sensitivity of the reaction to the form of the phosphorus source is surprising given that it might be expected that the addition of phosphorus pentoxide to water would result in instant hydrolysis to form orthophosphoric acid, and hence identical behavior in each case. Various possibilities were considered in trying to rationalize the differences seen in the two cases.

First, given the sensitivity of the reaction to the precise pH of solution and the difficulty of accurately weighing P_2O_5, it was considered possible that slight differences in the phosphorus stoichiometry of the reaction when phosphorus pentoxide was used were causing the formation of the intermediate phases. Therefore, reactions were performed in which orthophosphoric acid was used as the starting material, but the phosphorus stoichiometry was deliberately displaced slightly from the standard reaction composition. However, in all cases, ULM-5 crystallized smoothly from the reaction mixture and no intermediate phases were formed. Very high phosphorus stoichiometries led to the formation of condensed $GaPO_4$, and when very low phosphorus stoichiometries were used some unreacted Ga_2O_3 remained at the end of the reaction, but otherwise no differences in the reaction pathway were observed. It can therefore be concluded that the phosphorus stoichiometry is not a critical factor in the formation of the intermediate phases.

A second possibility considered was that it is simply the order of addition of the reagents which is important. In general, when orthophosphoric was used as the source material, it was added as an aqueous solution to the Ga_2O_3 *before* the addition of the amine template, whereas when phosphorus pentoxide was used, it was added *after* the amine. It was thought that this could cause different species to be formed in solution before reaction, leading to the differences in reaction pathway observed. To eliminate this possibility, reactions were performed in which orthophosphoric acid was added after the amine, and phosphorus pentoxide was added before the amine. No differences between these reactions and those performed previously were observed; i.e., no intermediates were seen in the former case, but were in the latter case, indicating that the order of addition of reagents is also not an important factor in the formation of the intermediates.

To completely exclude the possibility that the experimental procedure used was causing the differences seen in the two cases, a further experiment was performed in which P_2O_5 was added to water and the resulting solution stirred vigorously for 2 h, prior to addition to the other reagents and reaction. Even under these conditions it was observed that the reaction proceeded via the formation of intermediate phase(s). In other words, precisely the same behavior was observed as when P_2O_5 was added immediately prior to reaction. We therefore conclude that the marked difference in the reaction pathway observed in the two cases is not an artifact of the experimental procedure but reflects a fundamental difference in the phosphorus species

(48) Yu, L.; Pang, W.; Li, L. *J. Solid State Chem.* **1990**, *87*, 241−244.
(49) Ferey, G.; Loiseau, T.; Lacorre, P.; Taulelle, F. *J. Solid State Chem.* **1993**, *105*, 179−190.
(50) Taulelle, F. Personal communication.

present in solution during the crystallization. In particular, the addition of P_2O_5 to water does *not* result in the immediate formation of orthophosphoric acid.

One likely possibility is that the addition of P_2O_5 to water does not result in immediate complete hydrolysis to orthophosphoric acid, but instead results in the formation of oligomeric $[P_xO_{3x+1}]^{(n+2)-}$ polyphosphate species. Indeed, chain polyphosphates are well-known in solution, and it has been found that P−O−P linkages are kinetically stable toward hydrolysis in weakly acidic solutions at room temperature, where reaction half-lives can be on the order of years.[51] Oligomeric phosphate species could be expected to interact differently with the gallium and template species present in solution, forming precursor complexes which differ from those formed when only isolated phosphate units are present, and which favor the initial formation of intermediate phases on kinetic grounds.

Strong support for this idea is provided by an experiment performed in which the phosphorus source was replaced by polyphosphoric acid. Polyphosphoric acid is produced by dehydration of orthophosphoric acid and has the general formula $H_{n+2}P_nO_{3n+1}$; i.e., it contains exactly the sort of oligomeric phosphate units postulated to be formed on addition of P_2O_5 to water. Exactly the same behavior was observed during the synthesis as was observed in the P_2O_5 case, indicating that the presence of oligomeric phosphate units in solution does result in the formation of intermediate phases.

Further evidence in support of the presence of phosphate oligomers following the dissolution of P_2O_5 was provided by ex situ ^{31}P NMR studies of solutions of orthophosphoric acid, polyphosphoric acid, and phosphorus pentoxide dissolved in water. As expected, given that orthophosphoric acid is the primary standard for phosphorus NMR, its NMR spectrum consisted of a single singlet at 0 ppm. In contrast, ^{31}P NMR spectra of solutions of both polyphosphoric acid and phosphorus pentoxide dissolved in water displayed resonances at nonzero chemical shifts, consistent with the presence of phosphate oligomers in both solutions.

Difficulties in isolating pure samples of the intermediate phases, and reproducibility problems with the high-resolution in situ studies performed to date have hampered structural studies of the intermediate phases. Although high-resolution spectra of the two intermediates were obtained, the signal-to-noise ratio of these spectra is not sufficient to attempt a structure determination. Therefore, little definite can be said about the structures of the two intermediate phases at present.

Nevertheless, some thoughts on their likely structures can be proposed. One likely possibility is that the materials are layered phases containing two-dimensional gallophosphate sheets and interlamellar organic templates. Hypothetically, the two-dimensional layer structure could then transform directly to the three-dimensional structure via further condensation of the gallophosphate sheets. Such a transformation of two-dimensional layered structures to three-dimensional open-framework structures has been observed to occur during the synthesis of zeolite β,[52] and a direct solid-state transformation of a one-dimensional chain aluminophosphate to a two-dimensional layered aluminophosphate structure has been observed.[53] Such a possibility seems especially likely given the many structural relationships between the members of the ULM-*n* family.[15,16] ULM-3, -4, -5, -8, and -16 are all constructed from the same basic hexameric units, constructed from three PO_4 tetrahedra, two GaO_4F trigonal bipyramids, and one GaO_4F_2 octahedron connected via corner-sharing oxygen atoms. The different structures are formed by different connecting modes of these units with other hexameric units, or with other structural units. Of particular importance in the present discussion is the structural relationship between ULM-8 and ULM-5. ULM-8 is a layered material consisting of layers of corner-linked hexameric units separated by interlamellar organic cations.[54] Although ULM-5 is a fully connected three-dimensional material, it can be viewed as being constructed from very similar layers of corner-shared hexameric units which are then further connected via D4R (double four ring) octameric SBUs, forming the three-dimensional structure. Hypothetically, therefore, the intermediate phases observed could be two-dimensional structures similar to ULM-8 which contain gallophosphate layers constructed from hexameric units (although containing different interlamellar cations) which subsequently condense via the formation of bridging D4R units to form the final three-dimensional ULM-5 structure. Interestingly, recent in situ experiments we have performed on the syntheses of ULM-3, -4, and -16 have revealed that under certain experimental conditions these materials are also formed via crystalline intermediate phases. Given the structural relationships between these phases referred to above, this raises the fascinating possibility that the syntheses of these materials may proceed via structurally related phases, allowing one to build a coherent picture of their formation mechanisms. Since the presence of oligomeric phosphate species in solutions appears to influence the formation of the intermediate phases, a second possibility is that the intermediate phases contain P−O−P linkages in the form of corner-shared phosphate tetrahedra. No layered or microporous phosphates are presently known which contain corner-shared phosphate tetrahedra. However, there are several condensed metal phosphates which contain such units.

Efforts are continuing with regard to the determination of the composition and structures of the two intermediate phases. Given the difficulties in obtaining a pure sample of the intermediate phases for ex situ structure determination, any structural information will have to be obtained in situ. Two possibilities are currently being explored. First, further reactions using the high-resolution in situ facility at Brookhaven are planned. Given that the factors affecting the formation of one intermediate versus the other are now better understood, it should be possible to eliminate the problems of reaction irreproducibility and selectively force the formation of either intermediate at will. This will then enable the collection of high-quality XRD patterns of the materials. Second, Sankar and co-workers have described the development of a facility for obtaining simultaneous in situ XRD and EXAFS data on hydrothermal syntheses,[55] allowing one to correlate the formation of long-range ordered crystalline phases with short-range structural changes. We plan experiments using this facility to shed more light on the structural changes occurring during the formation of the intermediate and ULM-5 final product phases.

Conclusions

Using in situ energy and angular X-ray powder diffraction experiments, we have directly monitored, in real time, the

(51) Greenwood, N. N.; Earnshaw, A. *Chemistry of the Elements*; Pergamon Press Ltd.: Oxford, 1986; pp 595−602.

(52) Lohse, U.; Altrichter, B.; Fricke, R.; Pilz, W.; Schreier, E.; Garkisch, C.; Jancke, K. *J. Chem. Soc., Faraday Trans.* **1997**, *93*, 505−512.

(53) Oliver, S.; Kuperman, A.; Lough, A.; Ozin, G. A. *Chem. Mater.* **1996**, *8*, 2391−2398.

(54) Serpaggi, F.; Loiseau, T.; Riou, D.; Ferey, G. *Eur. J. Solid State Inorg. Chem.* **1994**, *31*, 595−604.

(55) Sankar, G.; Wright, P. A.; Natarajan, S.; Thomas, J. M.; Greaves, G. N.; Dent, A. J.; Dobson, B. R.; Ramsdale, C. A.; Jones, R. H. *J. Phys. Chem.* **1993**, *97*, 9550−9554.

structural changes occurring during the synthesis of ULM-5. The results of this study are a dramatic illustration both of the complexity of hydrothermal syntheses and of the power of in situ techniques to quickly and efficiently obtain unique information about the formation of microporous materials under normal laboratory reaction conditions.

The high time resolution and data quality that can be achieved using EDXRD has allowed us to accurately measure the rate of crystal growth over a wide range of temperature, pH, and source materials. This has enabled us to extract kinetic parameters and a model of the mechanism of ULM-5 crystallization. A combination of EDXRD and ADXRD techniques has been used to identify two previous unknown metastable intermediate phases during the formation of ULM-5 when phosphorus pentoxide is used as the phosphorus source. This is an important observation for its implications for the mechanism of ULM-5 formation, and one which could not have been obtained using conventional ex situ techniques.

Future work will concentrate on the important but difficult goal of determining the structures of the intermediate phases. A number of in situ techniques, such as combined EXAFS/XRD experiments, solution- and solid-state NMR experiments, and additional high-resolution angular dispersive diffraction experiments, will be used to gain structural information, and to further probe the growth mechanisms of the intermediate phases and their subsequent transformation to ULM-5.

Acknowledgment. We thank Dr. S. M. Clark and the technical staff at Daresbury Laboratory for assistance in the construction and operation of the hydrothermal cell, Dr. P. Norby and Dr. J. Hanson for assistance with the angular dispersive XRD experiments, and Dr. P. Rousell for collection of the ex situ ^{31}P NMR spectra. We also thank EPSRC and the Leverhulme trust for financial assistance. P.S.H. thanks Christ Church, Oxford, for a Junior Research Fellowship.

JA982441C